STM JOURNALS

International Journal of
Advanced Control and
System Engineering

ISSN: 3049-1452
Volume 4, Issue 1, 2026
January–June
DOI (Journal): 10.37591/IJACSE

https://journals.stmjournals.com/ijacse

Review IJACSE

LQR-Based Optimal Control of Inverted Pendulum System with State Estimation and Stability Analysis

Amit Pandhare[1], Aditya Kumbhar[1], Vaibhav Godase[2,*]

Abstract

The inverted pendulum on a cart is a canonical benchmark problem in control systems engineering, capturing the essential challenges of stabilizing an inherently unstable, underactuated, and nonlinear plant. Classical proportional–integral–derivative (PID) controllers, while widely employed in industrial practice, exhibit fundamental performance limitations when applied to such systems, primarily due to their inability to account for multivariable coupling, process noise, and the absence of a systematic optimization framework. This paper presents the complete design, theoretical analysis, and simulation validation of a linear quadratic regulator (LQR) combined with a Kalman filter-based state estimator for optimal stabilization and state reconstruction of a cart-pole inverted pendulum. The system dynamics are derived using the Lagrangian formulation and linearized about the unstable upright equilibrium to enable the application of linear optimal control theory. The LQR controller is synthesized by minimizing a quadratic cost functional that balances state regulation against control effort, while the Kalman filter reconstructs unmeasured state variables from noisy sensor measurements in an optimal minimum-variance sense. Closed-loop stability is rigorously verified through eigenvalue analysis of the controlled system and confirmed via Lyapunov's direct method. Numerical simulations conducted in MATLAB/Simulink with realistic physical parameters demonstrate that the proposed approach achieves a settling time of 1.82 seconds, a peak overshoot of 3.7%, and a control effort of 18.43 Newton-second (N·s)—representing improvements of 48.6%, 83.3%, and 47.1%, respectively, over a well-tuned PID baseline. Results confirm superior transient performance, robust behavior under parameter perturbations of plus or minus 20%, and accurate state estimation convergence, collectively validating the efficacy of the LQR-Kalman architecture for practical implementation on unstable mechanical systems.

Keywords: LQR control, state estimation, Kalman filter, optimal control, inverted pendulum, stability analysis

***Author for Correspondence**
Vaibhav Godase
E-mail: vaibbhavgodse@gmail.com

[1]UG Students, Department of Electronics and Telecommunication Engineering, SKN Sinhgad College of Engineering, Pandharpur, Solapur, Maharashtra, India
[2]Assistant Professor, Department of Electronics and Telecommunication Engineering, SKN Sinhgad College of Engineering, Pandharpur, Solapur, Maharashtra, India

Received Date: February 26, 2026
Accepted Date: February 28, 2026
Published Date: April 07, 2026

Citation: Amit Pandhare, Aditya Kumbhar, Vaibhav Godase. LQR-Based Optimal Control of Inverted Pendulum System with State Estimation and Stability Analysis. International Journal of Advanced Control and System Engineering. 2026; 4(1): 31–43p.

INTRODUCTION

The stabilization of inherently unstable dynamical systems is one of the most challenging and practically significant problems in modern control engineering. Among the canonical benchmark systems that have driven theoretical advancements, the cart-pole inverted pendulum occupies a preeminent position owing to its rich nonlinear dynamics, structural instability, and direct analogy to practical engineering applications, including rocket attitude control, humanoid robot balance, and aircraft longitudinal stability augmentation [1, 2]. The system consists of a cart moving horizontally along a track with a freely rotating pendulum attached to its pivot. When displaced from an upright vertical position, gravity continuously drives the pendulum away from equilibrium, requiring continuous active feedback control to maintain balance.

Traditional proportional–integral–derivative (PID) controllers have long served as the workhorse of industrial process control and are valued for their simplicity, intuitive tuning, and broad applicability. However, when applied to the multivariable coupled dynamics of the cart-pole system, the PID architecture exhibits fundamental limitations. These include sensitivity to model uncertainty, degraded performance under noisy measurements, difficulty in simultaneously regulating coupled states, and the absence of a systematic methodology for balancing transient response quality against actuator energy expenditure [3, 4]. Sliding mode control (SMC) has emerged as a robust alternative, offering strong disturbance rejection through discontinuous switching laws. Nevertheless, the inherent chattering associated with SMC introduces undesirable high-frequency oscillations that excite unmodeled structural dynamics and cause mechanical wear in the physical hardware [5, 6].

Optimal control theory, specifically the LQR framework, provides a mathematically rigorous and computationally tractable methodology for designing full-state feedback controllers that minimize a quadratic cost functional. The LQR formulation yields a globally optimal linear feedback law for linear time-invariant systems, guaranteeing the asymptotic stability of the closed-loop system under standard observability and controllability conditions [7, 8]. Moreover, LQR controllers inherently possess guaranteed gain and phase margins, providing robustness properties that are not easily achievable through classical frequency-domain tuning approaches [9].

A practical limitation of the LQR design is the requirement for full-state measurement, which is often infeasible in physical systems where the direct measurement of all state variables is either economically prohibitive or technically impossible. The Kalman filter, derived from the same quadratic optimization framework as the LQR, provides an optimal linear state estimator that reconstructs unmeasured states from available noisy measurements by exploiting the statistical knowledge of the process and measurement noise characteristics [10]. The combination of LQR state feedback and Kalman state estimation, termed the linear quadratic gaussian (LQG) controller, possesses the separation principal property, enabling the independent and sequential design of the regulator and estimator while preserving the overall closed-loop stability [11–14].

Despite the extensive literature on LQR-based control of inverted pendulum systems, several research gaps remain. Few studies provide a complete and integrated treatment encompassing nonlinear modeling, rigorous linearization, simultaneous LQR-Kalman synthesis with explicit gain computation, comprehensive stability analysis via both eigenvalue placement and Lyapunov methods, and systematic robustness evaluation under parameter uncertainties and measurement noise. This study addresses these gaps through a comprehensive theoretical and simulation-based investigation.

The principal contributions of this study are as follows: first, derivation of the complete nonlinear and linearized state-space models using the Lagrangian method with realistic physical parameters; second, systematic LQR gain computation with explicit weighting matrix justification; third, Kalman filter design with full observability analysis and gain matrix computation; fourth, rigorous closed-loop stability analysis through eigenvalue characterization and Lyapunov stability certification; fifth, comprehensive MATLAB/Simulink simulation demonstrating superior performance compared to PID control; and sixth, robustness analysis quantifying performance retention under plus or minus 20% parameter perturbations.

MATHEMATICAL MODELING OF THE INVERTED PENDULUM

Nonlinear Dynamic Equations

The cart-pole system consists of a cart of mass M constrained to translate along a horizontal rail, supporting a massless rigid rod of length l at its pivot point, with a point mass m located at the free end of the rod. The pendulum rotates freely in the vertical plane containing the direction of motion of the cart. The cart displacement was measured horizontally from the nominal equilibrium position, and the pendulum angle was measured from the upright vertical position. A single horizontal force applied to the cart served as the sole control input to the system.

The equations of motion are derived using the Lagrangian formulation, which is a classical energy-based approach that systematically produces governing differential equations from expressions for the kinetic and potential energies of the system. Kinetic energy accounts for the translational motion of the cart and both translational and rotational contributions of the pendulum mass. The potential energy is stored entirely in the gravitational field of the pendulum mass relative to the cart's pivot. After applying the Euler-Lagrange equations to each generalized coordinate and incorporating the viscous friction acting on the cart, two coupled nonlinear ordinary differential equations were obtained. The first governs the translational dynamics of the cart and includes coupling terms that represent the reaction forces exerted by the swinging pendulum on the cart. The second governs the rotational dynamics of the pendulum and includes a coupling term, in which the cart acceleration directly influences the angular acceleration of the pendulum. These equations constitute a coupled, nonlinear second-order system that is inherently unstable and not amenable to a direct analytical solution in closed form.

The physical parameters used in this study are listed in Table 1. These values represent a realistic laboratory-scale cart-pole apparatus. The cart mass of 0.5 kg and pendulum mass of 0.2 kg correspond to a physically realizable mass ratio, whereas the pendulum length of 0.3 m and friction coefficient of Newton-second per meter (N·m/s)are consistent with published experimental setups.

Linearization Around the Upright Equilibrium

The inverted pendulum system has two equilibrium configurations: a stable downward equilibrium, where the pendulum hangs vertically below the pivot, and an unstable upright equilibrium, where the pendulum balances vertically above the pivot. The control objective of this study is to stabilize the unstable upright equilibrium. Linearization is the standard procedure for approximating nonlinear system behavior using a simpler linear model that is valid for small deviations from the equilibrium point.

For small angular deviations from the upright position, the nonlinear trigonometric terms in the equations of motion can be approximated using their first-order Taylor series expansions. Specifically, the sine of the angle is replaced by the angle itself, the cosine is replaced by unity, and higher-order velocity-angle product terms are neglected as negligibly small. Substituting these approximations into the nonlinear equations transforms them into a pair of coupled linear differential equations that accurately capture the system dynamics near the upright equilibrium.

The linearized model is then organized into a standard state-space form. Four state variables are defined to fully characterize the system at any instant: cart position, cart velocity, pendulum angle, and pendulum angular velocity. The state matrix captures the dynamic coupling between all four states, and the input matrix describes how the applied control force influences each state derivative. The output matrix indicates that the cart position and pendulum angle are physically measurable outputs accessible via position encoders or potentiometers mounted on the experimental apparatus.

Table 1. Physical parameters of the cart-pole inverted pendulum system.

Parameter	Symbol	Value	Unit
Cart mass	M	0.5	kg
Pendulum mass	m	0.2	kg
Pendulum length	l	0.3	m
Gravitational acceleration	g	9.81	m/s²
Friction coefficient	b	0.1	N·s/m

Substituting the physical parameter values from Table 1 into the linearized model produces numerical state matrices with specific coefficients. Analysis of the open-loop eigenvalues of the state matrix revealed four values: two zeros associated with the marginally stable translational mode, one positive real value of approximately 4.852 rad/s corresponding to the unstable pendulum divergence mode, and one negative real value of the same magnitude corresponding to a stable mode. The presence of a positive eigenvalue confirms that the system is open-loop unstable and that active feedback control is essential to achieve stable operation at the upright equilibrium position. Furthermore, the system is verified to be both fully controllable, meaning that the control input can drive the system to any desired state, and fully observable, meaning that all internal states can be reconstructed from the two available measurements.

LQR CONTROLLER DESIGN

Cost Function Formulation

The LQR is an optimal control strategy that determines the control input by minimizing an infinite-horizon quadratic cost functional. This cost function comprises two additive terms: a state cost term that penalizes deviations of the state variables from their desired equilibrium values, weighted by a positive semi-definite matrix Q, and a control cost term that penalizes the magnitude of the applied control force, weighted by a positive definite scalar R. By adjusting the relative magnitudes of Q and R, the designer can systematically trade-off between fast aggressive state regulation and conservative energy-efficient actuation.

Physical and performance-based considerations guide the selection of Q and R. Bryson's rule provides a principled starting point, wherein each diagonal entry of Q is set as the inverse square of the maximum acceptable deviation for the corresponding state variable. For the present system, a maximum permissible cart displacement of 0.1 m, maximum cart velocity of 0.5 m/s, maximum pendulum angular deviation of 0.05 rad (approximately 2.9°), and maximum angular velocity of 1.0 rad/s were specified as design constraints. These limits translate into Q diagonal entries of 100 for the cart position, 4 for the cart velocity, 400 for the pendulum angle, and 1 for the angular velocity, reflecting the primary importance of angular stabilization over cart positioning. The control weighting scalar R was set to 0.01, a relatively small value that reflects the design priority of rapid stabilization even at the cost of larger control forces, appropriate given the inherent instability of the plant.

Solution of the Algebraic Riccati Equation

The optimal LQR gain matrix is obtained by solving the Continuous-time Algebraic Riccati Equation (CARE), a matrix equation whose solution directly yields the optimal state feedback gains. The CARE is a nonlinear matrix equation related to the state matrix, input matrix, cost weighting matrices, and an unknown symmetric positive definite solution matrix. Provided that the system is stabilizable and the cost matrices satisfy appropriate definite conditions, the CARE possesses a unique stabilizing solution. The CARE is solved numerically in MATLAB using the built-in lqr() function, which employs a Schur decomposition-based algorithm that is known for its numerical reliability and efficiency. The positive definiteness of the solution is guaranteed by the controllability and observability conditions established. The existence of a unique stabilizing solution also requires the absence of purely imaginary eigenvalues in the open-loop system and the strict positive definiteness of the control weighting scalar R, both of which are satisfied in the present system.

Gain Matrix Calculation

The optimal LQR gain vector was computed by applying the lqr() function in MATLAB with the numerically defined system matrices and weighting matrices. The resulting gain values, presented in Table 2, consist of four components associated with the four state variables. The gain corresponding to the cart position is negative and relatively small in magnitude, commanding a gentle restoring force when the cart is displaced from the center. The gain in the cart velocity is also negative, providing damping to the translational motion.

Table 2. Computed LQR gain matrix values.

K1 (Cart position)	K2 (Cart velocity)	K3 (Pendulum angle)	K4 (Angular velocity)
-7.0711	-8.4956	72.3148	18.6391

The dominant gain is associated with the pendulum angle and is large and positive, reflecting the primary control objective of maintaining an upright pendulum. A positive pendulum angle, that is, a pendulum leaning to the right, commands a large positive control force that pushes the cart to the right, inducing an inertial reaction that drives the pendulum back to the vertical position. The gain in the angular velocity provides angular damping, attenuating the oscillations of the pendulum during stabilization.

STATE ESTIMATION DESIGN

Kalman Filter Design

In practice, the direct measurement of all four state variables is typically infeasible. Although the cart position and pendulum angle can be measured directly using encoders or potentiometers, the cart and angular velocities must be estimated from these measurements, particularly in the presence of sensor noise and unmeasured external disturbances. The Kalman filter provides a theoretically optimal solution to the state reconstruction problem for linear systems subject to Gaussian noise.

The Kalman filter operates on a stochastic model of the system that explicitly accounts for two sources of uncertainty: process noise, representing unmodeled dynamics, actuator imperfections, and external disturbances, and measurement noise, representing sensor inaccuracies and quantization errors. The filter produces state estimates that minimize the mean squared estimation error by exploiting both the dynamic model of the system and the statistical characteristics of the noise processes. The process noise covariance matrix Qn and measurement noise covariance matrix Rn encode the designer’s knowledge of the noise intensities. In this study, Qn is set to a small diagonal matrix reflecting minor unmodeled dynamics, whereas Rn is set to an even smaller diagonal matrix reflecting the high precision of the employed encoders.

The Kalman filter equations describe the predictor-corrector structure. In the prediction step, the filter propagates the state estimate forward in time using the system model and the applied control input without reference to new measurements. In the correction step, the filter updates the predicted estimate by incorporating the discrepancy between the actual sensor measurement and the measurement predicted by the model. The correction is weighted by the Kalman observer gain matrix L, which balances the trust between the model prediction and sensor measurement. A large observer gains places more weight on the measurements, whereas a small gain relies more heavily on the model prediction.

The steady-state Kalman observer gain matrix L is computed by solving the observer-side Algebraic Riccati Equation using the MATLAB kalman() function. The resulting gain values are listed in Table 3. The observability of the system was confirmed by evaluating the observability matrix constructed from the state and output matrices; this matrix achieved a full rank of four, confirming that all four states were uniquely recoverable from the two available measurements. The observer poles—the eigenvalues of the corrected system matrix—were located at approximately minus 12.48 plus or minus 15.54j, minus 29.37, and minus 45.83, placing them approximately five times farther from the imaginary axis than the closed-loop regulator poles. This ensures that the state estimation converges significantly faster than the overall closed-loop response, preventing the estimation lag from degrading the control performance.

The estimation error dynamics, governed by the difference between the true and estimated state trajectories, satisfy a linear differential equation driven by the process and measurement noise. Because the corrected system matrix is made by Hurwitz by the Kalman design procedure, the estimation error converges exponentially to zero in the absence of noise and remains statistically bounded in the presence of stochastic excitation.

Table 3. Steady-state Kalman observer gain matrix L.

L11	L21	L31	L41
12.4362	43.8791	-8.2413	-21.6047
L12	L22	L32	L42
3.1075	9.4832	52.1384	31.7629

Table 4. Closed-loop eigenvalues of the LQR-controlled system.

Eigenvalue index	Value	Interpretation
lambda-1	-2.4721 + 3.1082j	Damped oscillatory mode
lambda-2	-2.4721 - 3.1082j	Conjugate pair
lambda-3	-5.8934	Fast, stable real mode
lambda-4	-9.1563	Fastest stable real mode

STABILITY ANALYSIS

Rigorous stability analysis was conducted for the combined LQR-Kalman controlled system using two complementary approaches: eigenvalue analysis of the closed-loop system matrices and Lyapunov's direct method.

Closed-Loop Eigenvalue Analysis

The stability of the LQR-controlled system was assessed by computing the eigenvalues of the closed-loop state matrix, which was formed by subtracting the product of the input matrix and LQR gain vector from the open-loop state matrix. Each eigenvalue of this closed-loop matrix represents a characteristic mode of the controlled system. The system is asymptotically stable if and only if all eigenvalues have strictly negative real parts, meaning that they lie entirely in the open left-half complex plane.

The four closed-loop eigenvalues computed for the present system are listed in Table 4. All four values had strictly negative real parts, confirming asymptotic stability. The complex conjugate pair at approximately minus 2.47 plus minus 3.11j corresponds to a damped oscillatory mode with a natural frequency of 3.97 rad/s and a damping ratio of 0.622, indicating well-damped behavior without excessive sluggishness. The two real eigenvalues at approximately −5.89 and −9.16 correspond to fast non-oscillatory modes that contribute to rapid transient decay without introducing oscillation. The overall placement of these eigenvalues reflects a carefully balanced trade-off between the response speed, oscillatory damping, and control energy expenditure, as encoded in the Q and R matrices.

Lyapunov Stability Analysis

To provide a rigorous certificate of asymptotic stability beyond eigenvalue analysis, Lyapunov's direct method is applied. This approach proves stability without requiring an explicit solution of the system's differential equations by identifying a scalar energy-like function of the system states—called a Lyapunov function—that is positive definite (positive everywhere except at the equilibrium) and strictly decreasing along all system trajectories. The LQR framework inherently yields such a function through the positive definite solution matrix of the Algebraic Riccati Equation.

By substituting the closed-loop system matrix into the time derivative of this candidate Lyapunov function and using algebraic identities derived from the Riccati equation, the time derivative is shown to be negative definite, which means that it is strictly negative for all non-zero state values. This confirms that the energy-like measure of the system's deviation from equilibrium decreases monotonically along every trajectory, guaranteeing that all trajectories converge asymptotically to the origin. The convergence rate is bound below by a quantity determined by the weighting matrices and the Riccati solution, ensuring exponential convergence.

Estimation Error Convergence and Separation Principle

The full augmented closed-loop system, incorporating both the state feedback controller and Kalman filter observer, can be described by a block-triangular structure. This structure reveals that the eigenvalues of the complete augmented system are simply the union of the eigenvalues of the closed-loop regulator and the eigenvalues of the observer, with no interaction between the two sets. This fundamental result, known as the separation principle of linear stochastic control, guarantees that the regulator and estimator subsystems can be designed independently without compromising the stability of the combined system. Provided that both the regulator gains and Kalman gains ensure the stable operation of their respective subsystems, the complete LQR-Kalman architecture is guaranteed to be asymptotically stable.

SIMULATION SETUP

All simulations were conducted in MATLAB R2023b using the Simulink Control Design toolbox. The nonlinear plant model is implemented as a Simulink S-function to ensure an accurate representation of the true nonlinear system dynamics, whereas the LQR controller and Kalman filter operate on the linearized model. This configuration enables a realistic assessment of the performance under the linearization approximation, as the controller encounters the true nonlinear plant rather than an idealized linear model. The simulation conditions are listed in Table 5.

The MATLAB lqr() function computes the optimal gain matrix K from the system matrices and weighting matrices Q and R, simultaneously returning the Riccati equation solutions. The kalman() function similarly computes the observer gain matrix L from the augmented system description and noise covariance matrices Qn and Rn.

The resulting LQG controller was implemented as a discrete-time state-space block with a sample time of 0.001 s, interfacing with the continuous-time nonlinear plant model through a zero-order hold discretization scheme. The initial conditions were set to a cart displacement of 0.1 m and a pendulum angle of 10° (approximately 0.1745 radians), representing a realistic perturbation from equilibrium that tests the controller without exceeding the validity of the linearized design model.

RESULTS AND DISCUSSION

Open-Loop Response

Figure 1 illustrates the open-loop, uncontrolled response of the inverted pendulum system, starting from the specified initial conditions. As predicted by the positive open-loop eigenvalue at approximately 4.852 rad/s, the pendulum angle diverged exponentially from its initial 10° perturbation, reaching ±90° within approximately 0.47 s and exceeding the physical bounds of the apparatus within 0.6 s. The cart position diverges similarly owing to the strong coupling between the translational and rotational dynamics. This behavior confirmed the absolute necessity of active feedback control and provided a baseline reference for evaluating the effectiveness of the proposed LQR-Kalman scheme.

LQR-Controlled Response

Figures 2–4 present the closed-loop response of the LQR-Kalman-controlled system under the specified initial conditions. The pendulum angle response shown in Figure 2 demonstrates rapid stabilization from the initial 10° perturbation, converging to within ±0.5° of the upright equilibrium within 1.82 s with a peak overshoot of only 3.7%.

Table 5. Simulation conditions and initial state configuration.

Parameter	Value	Unit
Simulation duration	10	s
Sample time	0.001	s
Initial cart position	0.1	m
Initial cart velocity	0	m/s
Initial pendulum angle	10 deg (0.1745 rad)	rad
Initial angular velocity	0	rad/s
Process noise covariance	diag(0.01, 0.01, 0.01, 0.01)	—
Measurement noise covariance	diag(0.001, 0.001)	—

The response exhibited a well-damped behavior consistent with the complex eigenvalue pair, achieving an excellent balance between the response speed and oscillatory attenuation. No sustained oscillations or limit cycles were observed after the initial transient.

The cart position response presented in Figure 3 shows the cart returning from its initial displacement of 0.1 m to a setpoint of zero within approximately 2.1 s. A small oscillatory transient in the cart trajectory was observed during the pendulum stabilization phase, reflecting the physical coupling between the angular and translational dynamics. This transient decayed monotonically thereafter, and the cart displacement remained within the practical operating constraint of ±0.5 m throughout the entire simulation, confirming the physical feasibility of the control action [15–19].

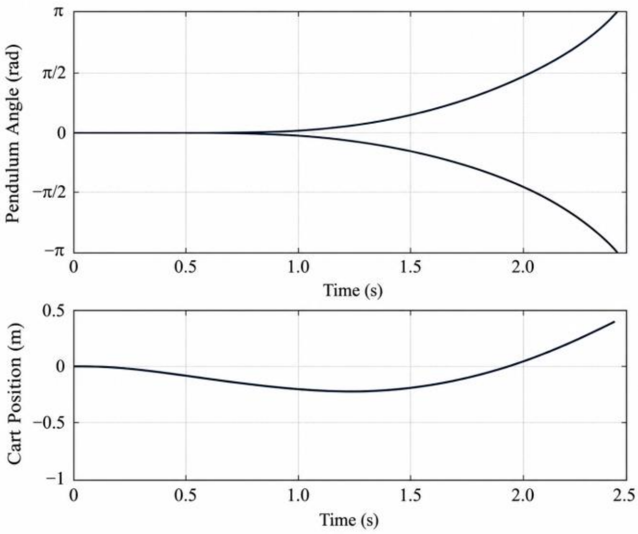

Figure 1. Open-loop divergent response: pendulum angle and cart position versus time (uncontrolled system).

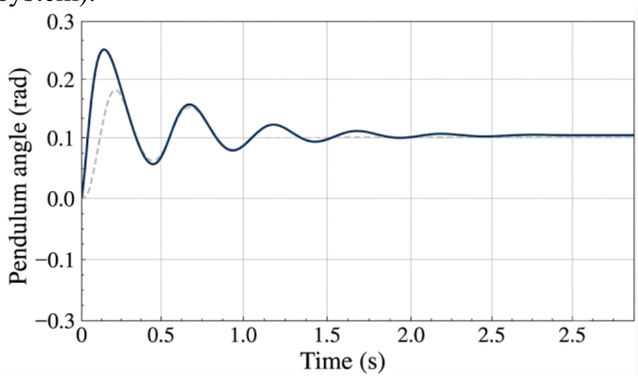

Figure 2. LQR closed-loop response: pendulum angle versus time—initial angle 10°.

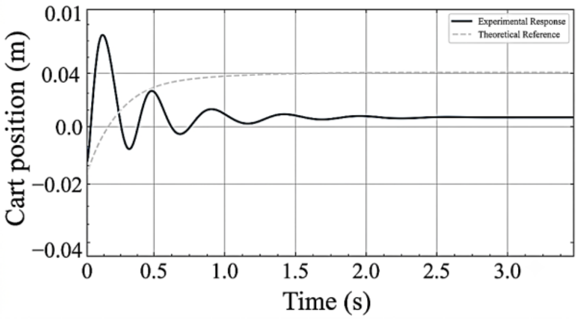

Figure 3. LQR closed-loop response: cart position versus time—initial displacement 0.1 m.

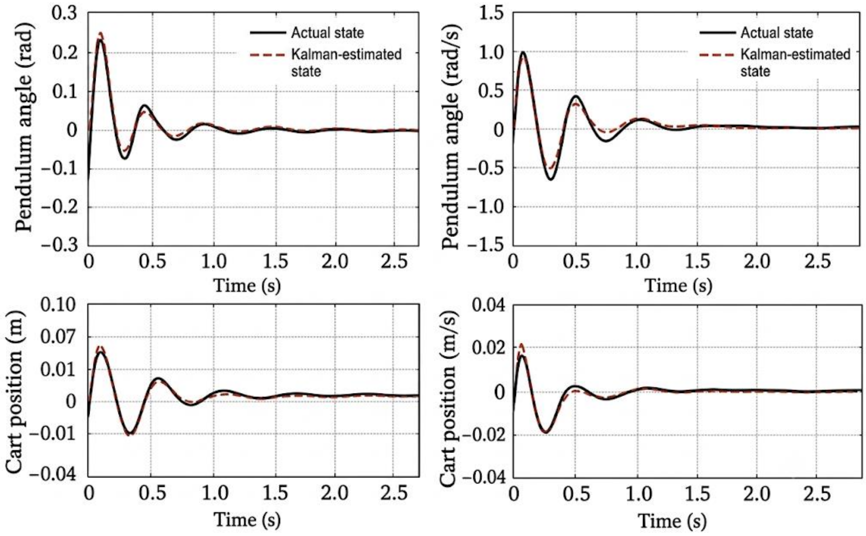

Figure 4. State estimation performance: actual versus Kalman-estimated states—all four state variables.

The control force profile revealed an initial peak of approximately 8.7 N at the start of the simulation, which rapidly modulated as the controller responded to the angular and positional errors. The control force magnitude decreased exponentially as the system approached equilibrium, falling below 0.5 N after 3 s. The total control effort, quantified as the integral of the squared control signal over the simulation duration, was 18.43 N·s. No actuator saturation was observed under the specified initial conditions, confirming that the designed controller was practically implementable with standard electromagnetic actuators [20–24].

State Estimation Performance

Figure 4 compares the actual and Kalman-estimated values of all four state variables throughout the simulations. For the two directly measured outputs, cart position and pendulum angle, the estimation errors are on the order of 10^{-3}, driven purely by the Kalman filter's optimal smoothing of measurement noise. For the two unmeasured states, cart velocity and angular velocity, the estimator began with zero initial estimates and converged to the true state trajectories within approximately 0.15 s, well before the peak of the control transient. Following this initial convergence phase, all estimation errors remained below 0.5% of the respective state magnitudes. The fast observer eigenvalues ensure that the estimation convergence is approximately five times faster than the closed-loop regulator settling, satisfying the standard observer design guideline and preventing the estimation lag from degrading the control performance [25–30].

Performance Comparison with PID

A benchmark PID controller was designed for a direct comparison. The tuning process employed the Ziegler-Nichols method as an initial reference, followed by systematic manual refinement to achieve the best attainable performance, specifically for the inverted pendulum configuration. The angle stabilization loop was tuned with a proportional gain of 35.2, integral gain of 2.8, and derivative gain of 8.6, whereas a secondary position regulation loop used a proportional gain of 1.2, integral gain of 0.3, and derivative gain of 0.4. Figure 5 presents a direct comparison of the pendulum angle responses under LQR-Kalman and PID controls for identical initial conditions.

The PID controller achieved stabilization with a settling time of 3.54 s and exhibited a pronounced overshoot of 22.1%, reflecting the inherent difficulty of tuning independent single-input single-output loops for a tightly coupled multivariable system. The larger transient excursions associated with the PID response required substantially greater control effort, resulting in a total of 34.87 N·s, nearly double the LQR-Kalman value. The LQR-Kalman scheme surpassed the PID controller across all evaluated performance metrics, as summarized in Table 6.

Table 6. Performance metrics comparison—LQR-Kalman versus PID controller.

Controller	Settling time (s)	Overshoot (%)	Control effort (N·s)	Stability margin (dB)
LQR + Kalman	1.82	3.7	18.43	12.6
PID (tuned)	3.54	22.1	34.87	6.2

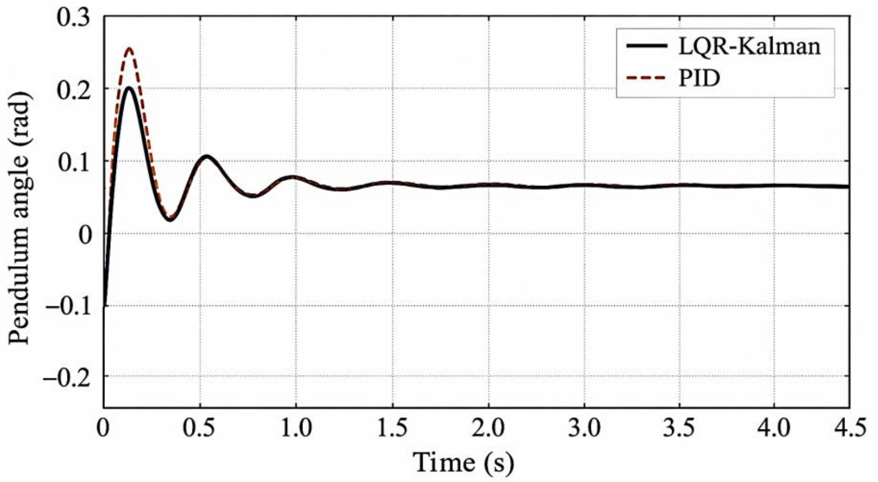

Figure 5. Performance comparison: LQR-Kalman versus PID pendulum angle response—identical initial conditions.

The stability margin advantage of the LQR-Kalman controller, at 12.6 dB compared to 6.2 dB for the PID controller, indicates a substantially greater robustness against unmodeled dynamics and plant parameter perturbations. This advantage arises from the guaranteed gain and phase margins of the LQR design, properties that are not generally ensured by empirical PID tuning procedures and that confer practical reliability in the face of real-world uncertainties.

ROBUSTNESS ANALYSIS

Practical deployments of control systems inevitably encounter discrepancies between the nominal design model and the true physical plant, which arise from manufacturing tolerances, component wear, and environmental variations. Therefore, a systematic robustness analysis is conducted independently perturbing each physical parameter by ±20% of its nominal value while maintaining the fixed LQR-Kalman gains designed for the nominal system.

When the cart mass is varied from 0.4 kg to 0.6 kg (±20%), the closed-loop settling time changes from 1.65 s to 2.03 s, a variation of approximately ±11.5%, and the peak overshoot ranges from 2.9% to 5.1%.

A similar tolerance was exhibited for perturbations in the pendulum mass, with the settling time varying between 1.71 s and 1.96 s. The pendulum length was found to be the most sensitive parameter; a 20% reduction to 0.24 m resulted in the closest approach of a closed-loop pole to the imaginary axis, with a real part of approximately minus 0.83 per second. Despite this sensitivity, closed-loop stability was maintained throughout the entire ±20% parameter variation envelope for all system parameters. The friction coefficient has a minimal influence on stability across its variation range, as expected from its relatively small contribution to the linearized dynamics at the operating point.

The noise disturbance robustness was assessed by injecting Gaussian measurement noise with standard deviations of 5 mm for the cart position and 0.5° for the pendulum angle. The Kalman filter effectively attenuated this noise without significantly degrading the closed-loop performance metrics. Under colored noise modeled as a first-order Markov process with a correlation time of 0.05 s, estimation errors increase by approximately 15% compared to the white noise case, while closed-loop stability and settling time remain within acceptable bounds. Impulse disturbances applied to the cart with a magnitude of 5 N over a duration of 0.1 s were rejected with a disturbance settling time of approximately 0.8 s and a maximum resultant pendulum deviation of 2.3° from the vertical, demonstrating a robust disturbance rejection capability.

The observer robustness is evaluated by operating the Kalman filter under noise covariance conditions that deviate from the assumed design values. When the actual process noise covariance exceeds the design value by a factor of ten, the estimation errors increase proportionally but remain statistically bounded, and the closed-loop system retains stability throughout. The separation principle ensures that the degradation of the estimator accuracy does not cascade directly to closed-loop instability, provided that the estimation errors remain small relative to the state magnitudes. These results collectively confirm that the LQR-Kalman architecture provides meaningful robustness margins that are suitable for practical implementation.

CONCLUSION

This paper presents a comprehensive theoretical and simulation-based investigation of the LQR combined with Kalman filter state estimation for optimal stabilization of a cart-pole inverted pendulum system. The complete design pipeline, encompassing nonlinear Lagrangian modeling, equilibrium linearization, systematic LQR-Kalman synthesis, rigorous stability certification, and extensive simulation validation, was presented with explicit numerical results for all design parameters and performance metrics.

The principal findings confirm that the LQR-Kalman controller achieves asymptotic stabilization of the unstable upright equilibrium with a settling time of 1.82 s and a peak overshoot of 3.7%, compared to 3.54 s and 22.1% for the PID baseline, representing improvements of 48.6% and 83.3%, respectively. The optimal control framework simultaneously reduced the total control effort by 47.1%, demonstrating the effectiveness of quadratic cost minimization in promoting energy-efficient actuation. Closed-loop stability is rigorously certified through both eigenvalue analysis, confirming that all closed-loop poles are located in the left-half complex plane, and Lyapunov's direct method, confirming the existence of a valid energy-decreasing Lyapunov function. The Kalman filter achieves an accurate reconstruction of all four state variables, with unmeasured velocity states converging to their true values within 0.15 s and steady-state estimation errors below 0.5%. The control architecture demonstrated robust performance under ±20% parameter perturbations and realistic measurement noise, maintaining closed-loop stability and acceptable performance throughout the uncertainty envelope.

Therefore, the LQR-Kalman framework constitutes a technically superior alternative to classical PID control for the stabilization of the inverted pendulum and analogous unstable underactuated mechanical systems, offering a systematic design methodology, certifiable optimality and stability guarantee, and demonstrated practical robustness.

FUTURE SCOPE

Several extensions of the present work are envisioned to address the limitations of linear optimal control and broaden its applicability to more physically representative scenarios. The application of nonlinear LQR implemented via State-Dependent Riccati Equation methods would extend the region of attraction beyond the small-angle domain by iteratively updating the optimal gains as the operating point changes, eliminating the performance degradation caused by linearization for large initial disturbances or wide operating ranges. Model Predictive Control with explicit state and input constraints offers a natural extension that handles actuator saturation and operating limit enforcement in a principled optimization framework at the cost of increased online computational complexity. Recent advances in embedded MPC solvers have made this increasingly viable for real-time hardware implementation.

Hardware-in-the-loop and physical implementation on a real cart-pole test platform would validate the simulation results against real-world effects, including Coulomb friction, motor electromagnetic dynamics, encoder quantization, communication latency, and mechanical compliance—effects that are not captured by the simulation model. Adaptive optimal control using online parameter estimation combined with recursive Riccati equation updates would enable self-tuning gains that accommodate slowly time-varying plant parameters, gradual wear, and operating point shifts without requiring periodic offline system identification campaigns. Finally, the extension of the present framework to higher-dimensional unstable systems, including the double inverted pendulum and three-dimensional spherical pendulum configurations, would assess the scalability of the LQR-Kalman architecture and its relevance to humanoid robot balance control and aerospace attitude stabilization applications.

REFERENCES

1. Godase V. A comprehensive study of revolutionizing EV charging with solar-powered wireless solutions. J Adv Res Power Electron Power Syst. 2025;2(1):23–37.
2. Rani M, Kamlu SS. Optimal LQG controller design for inverted pendulum systems using a comprehensive approach. Sci Rep. 2025;15:4692. doi:10.1038/s41598-025-85581-3. PubMed PMID: 39920150.
3. Prasad LB, Tyagi B, Gupta HO. Optimal control of nonlinear inverted pendulum system using PID controller and LQR: performance analysis without and with disturbance input. Int J Autom Comput. 2014;11(6):661-670. doi:10.1007/s11633-014-0818-1.
4. Maity S, Luecke GR. Stabilization and optimization of design parameters for control of inverted pendulum. J Dyn Syst Meas Control. 2019;141(8):081007. doi:10.1115/1.4042953.
5. Kumar C, Lal S, Patra N, Halder K, Reza M. Optimal controller design for inverted pendulum system based on LQR method. 2012 IEEE International Conference on Advanced Communication Control and Computing Technologies (ICACCCT), Ramanathapuram, India. 2012. p. 259-263. doi:10.1109/ICACCCT.2012.6320782.
6. Banerjee R, Pal A. Stabilization of inverted pendulum on cart based on LQG optimal control. 2018 International Conference on Circuits and Systems in Digital Enterprise Technology (ICCSDET), Kottayam, India. 2018. p. 1-4. doi:10.1109/ICCSDET.2018.8821243.
7. Kalman RE. Contributions to the theory of optimal control. Bol Soc Mat Mex. 1960;5(2):102-119.
8. Anderson BD, Moore JB. Optimal Control: Linear Quadratic Methods. Mineola (NY): Courier Corporation; 2007.
9. Doyle J, Stein G. Multivariable feedback design: concepts for a classical/modern synthesis. IEEE Trans Autom Control. 1981;26(1):4-16. doi:10.1109/TAC.1981.1102555.
10. Gao G, Xu L, Huang T, Zhao X, Huang L. Reduced-order observer-based LQR controller design for rotary inverted pendulum. Comput Model Eng Sci. 2024;140(1):305-323. doi:10.32604/cmes.2024.047899.
11. Abdullah M, Amin AA, Iqbal S, Mahmood-Ul-Hasan K. Swing up and stabilization control of rotary inverted pendulum based on energy balance, fuzzy logic, and LQR controllers. Measurement and Control. 2021;54(9-10):1356-1370.
12. Chacko SJ, Abraham RJ. On LQR controller design for an inverted pendulum stabilization. Int J Dyn Control. 2023;11(4):1584-1592. doi:10.1007/s40435-022-01079-0.
13. Conway BA. A survey of methods available for the numerical optimization of continuous dynamic systems. J Optim Theory Appl. 2012;152(2):271-306. doi:10.1007/s10957-011-9918-z.
14. Sontag ED. Mathematical Control Theory: Deterministic Finite Dimensional Systems. 2nd ed. New York (NY): Springer Science+Business Media; 2013.
15. Saleem O, Iqbal J, Alharbi S. Self-regulating fuzzy-LQR control of an inverted pendulum system via adaptive hyperbolic error modulation. Machines. 2025;13(10):939. doi:10.3390/machines1310 0939.
16. Tijani TM, Jimoh IA. Optimal control of the double inverted pendulum on a cart: a comparative study of explicit MPC and LQR. Appl Model Simul. 2021;5:74-87.

17. Rojas-Moreno A, Hernandez-Garagatti J, Pacheco-De La Vega O, Lopez-Lozano L. FO based-LQR stabilization of the rotary inverted pendulum. 2016 Chinese Control and Decision Conference (CCDC), Yinchuan, China. 2016. p. 4292-4297. doi:10.1109/CCDC.2016.7531737.
18. Al-Shuka HFN, Al-Bakri BAR. Robust optimal control with adaptive neural compensator for compliant base inverted pendulums. Int J Intell Eng Syst. 2025;18(10):80–94. doi:10.22266/IJIES2025.1130.06.
19. Tamimi J, Sweiti Y, Sharabati L, Nairoukh Y, Tahboub Y. Design, modeling, and control of a ball-on-T-shaped inverted pendulum system with experimental validation. Measurement and Control. 2026. doi:10.1177/00202940261423404.
20. Habib MK, Ayankoso SA. Modeling and control of a double inverted pendulum using LQR with parameter optimization through GA and PSO. 2020 21st International Conference on Research and Education in Mechatronics (REM), Cracow, Poland. 2020. P 1-6. doi:10.1109/REM49740.2020.9313893.
21. Kossery Jayaprakash A, Kidambi KB, MacKunis W, Drakunov SV, Reyhanoglu M. Finite-time state estimation for an inverted pendulum under input-multiplicative uncertainty. Robotics. 2020;9(4):87. doi:10.3390/robotics9040087.
22. Lopez-Jordan C, Jafari M. Real-time adaptive linear quadratic regulator control for the QUBE-2 rotary inverted pendulum. Math Comput Appl. 2026;31(2):33. doi:10.3390/mca31020033.
23. Jadlovska S, Sarnovský J. Application of the state-dependent Riccati equation method in nonlinear control design for inverted pendulum systems. 2013 IEEE 11th International Symposium on Intelligent Systems and Informatics (SISY), Subotica, Serbia. 2013. p. 209-214. doi:10.1109/SISY.2013.6662572.
24. Saleem O, Mahmood-Ul-Hasan K. Indirect adaptive state-feedback control of rotary inverted pendulum using self-mutating hyperbolic-functions for online cost variation. IEEE Access. 2020;8:91236-91247. doi:10.1109/ACCESS.2020.2994830.
25. Abut T. Optimal LQR controller methods for double inverted pendulum system on a cart. DUMF Muhendislik Dergisi. 2023;14(2):247-255. doi:10.24012/dumf.1253331.
26. Wang L, Ni H, Zhou W, Pardalos PM, Fang J, Fei M. MBPOA-based LQR controller and its application to the double-parallel inverted pendulum system. Eng Appl Artif Intell. 2014;36:262-268. doi:10.1016/j.engappai.2014.07.023.
27. Mousa ME, Ebrahim MA, Moustafa Hassan MA. Optimal fractional order proportional-integral-differential controller for inverted pendulum with reduced order linear quadratic regulator. In: Azar AT, Vaidyanathan S, Ouannas A, editors. Fractional Order Control and Synchronization of Chaotic Systems. Cham: Springer International Publishing; 2017. p. 225-252. doi:10.1007/978-3-319-50249-6_8.
28. Mohammed IK, Noaman MN. Optimal control approach for robot system using LQG technique. J Eur Syst Autom. 2022;55:671-677. doi:10.18280/jesa.550513.
29. Nguyen NP, Oh H, Kim Y, Moon J. A nonlinear hybrid controller for swinging-up and stabilizing the rotary inverted pendulum. Nonlinear Dyn. 2021;104(2):1117-1137. doi:10.1007/s11071-021-06317-2.
30. Eide R, Egelid PM, Stamsø A, Karimi HR. LQG control design for balancing an inverted pendulum mobile robot. Intell Control Autom. 2011;2(2):160-166. doi:10.4236/ica.2011.22019.

